

Title Page

Full Title

Automatic classification between COVID-19 pneumonia, non-COVID-19 pneumonia, and the healthy on chest X-ray image: combination of data augmentation methods in a small dataset

Authors and Affiliations

Mizuho Nishio, MD, PhD¹, Shunjiro Noguchi, MD², Hidetoshi Matsuo, MD¹, Takamichi Murakami, MD, PhD¹

1 Department of Radiology, Kobe University Graduate School of Medicine, 7-5-2 Kusunoki-cho, Chuo-ku, Kobe 650-0017 JAPAN

2 Department of Diagnostic Imaging and Nuclear Medicine, Kyoto University Graduate School of Medicine, 54 Shogoin Kawaharacho, Sakyo-ku, Kyoto, 606-8507, Japan

*Corresponding author: Mizuho Nishio, MD, PhD

Department of Radiology, Kobe University Graduate School of Medicine, 7-5-2

Kusunoki-cho, Chuo-ku, Kobe 650-0017 JAPAN

Tel.: +81-78-382-6104. Fax: +81-78-382-6129

e-mail: nishiomizuho@gmail.com

Abstract

Purpose: To develop and validate computer-aided diagnosis (CADx) system for classification between COVID-19 pneumonia, non-COVID-19 pneumonia, and the healthy on chest X-ray (CXR) images. Because CXR datasets related with COVID-19 were small, transfer learning with pretrained models and combination of data augmentation methods were used to improve accuracy and robustness of the CADx system.

Materials and Methods: From two public datasets, 1248 CXR images were obtained, which included 215, 533, and 500 CXR images of COVID-19 pneumonia, non-COVID-19 pneumonia, and the healthy. The proposed CADx system utilized VGG16 as a pretrained model and combination of conventional method and mixup as data augmentation methods. Other types of pretrained models were used for comparison with the VGG16-based model. In addition, single type or no data augmentation methods were also evaluated. Splitting of training/validation/test sets was used when building and evaluating the CADx system. Three-category accuracy was evaluated for test set with 125 CXR images.

Results: The three-category accuracy of the CAD system was 83.6% between COVID-19 pneumonia, non-COVID-19 pneumonia, and the healthy. In addition, sensitivity of

COVID-19 pneumonia was more than 90%. The combination of conventional method and mixup was more useful than single type or no data augmentation methods.

Conclusions: It was possible to build the accurate CADx system for the 3-category classification of COVID-19 pneumonia, non-COVID-19 pneumonia, and the healthy.

Keywords: chest X-Ray image; deep learning; data augmentation; COVID-19

Introduction

Outbreak of novel coronavirus disease (COVID-19) started in Wuhan, Hubei province, China at the end of 2019 ¹, and COVID-19 spread across the world in 2020. COVID-19 is caused by a strain of coronavirus called the Severe Acute Respiratory Syndrome Coronavirus 2 (SARS-CoV-2) ². The World Health Organization declared COVID-19 as a pandemic on March 11, 2020 ³. COVID-19 can be detected with the use of real-time polymerase chain reaction (RT-PCR) tests of SARS-CoV-2. Although specificity of RT-PCR was sufficiently high for COVID-19, its sensitivity was relatively low in detecting COVID-19 ⁴. Chest computed tomography (CT) was useful for detecting abnormal findings of COVID-19 pneumonia, and the findings of COVID-19 pneumonia was characterized by ground glass opacity which was distributed predominantly on lung peripherals ^{4,5}. The CT findings of COVID-19 could be regarded as distinct from viral pneumonia and bacterial pneumonia.

Although usefulness of CT for detecting COVID-19 pneumonia was shown in several studies, CT is not suitable for COVID-19 screening due to its cost and radiation exposure ⁶. From the view point of screening, chest X-Ray imaging (CXR) is cost effective and commonly used for screening purpose. CXR findings of COVID-19 pneumonia was characterized by the followings; consolidation was the most common

finding, followed by ground glass opacity; distribution of CXR abnormalities could be peripheral and lower zone distribution with bilateral involvement; pleural effusion was uncommon⁷. Compared with chest CT, sensitivity of CXR is generally low for pulmonary diseases. Therefore, accurate diagnosis of COVID-19 pneumonia can be more challenging on CXR than on chest CT.

Computer-aided diagnosis (CADx) is being used for detection and diagnosis in several medical fields. CADx utilizes artificial intelligence methods for improving its diagnostic accuracy and robustness. Recently, advances in machine learning, particularly deep learning with convolutional neural network (CNN), have shown promising performance of CADx in classifying disease patterns on medical images, such as CXR and chest CT⁸⁻¹¹.

The purpose of the current study was to develop CADx system for classification between COVID-19 pneumonia, non-COVID-19 pneumonia, and the healthy using CXR images and CNN. Because the number of publicly available CXR images of COVID-19 pneumonia was limited, we developed the CNN model which could be accurate and robust even if the training data of CNN was small. The proposed method was characterized by the following two points. One is the transfer learning, in which CNN models pretrained on a large dataset are used for improvement of accuracy and robustness

^{9,12}. Although the current study mainly utilized a commonly-used pretrained model (VGG16), the latest CNN model (EfficientNet) was also used for the transfer learning. Next, combination of data augmentation methods was used for improving model's robustness. In addition to conventional data augmentation method (such as flipping, shifting, rotating, and etc.), mixup, and Random Image Cropping and Patching (RICAP) were used in the current study ¹³⁻¹⁵. The model obtained by the proposed method was examined to evaluate whether the model exhibited sufficient performance of the COVID-19 pneumonia against both non-COVID-19 pneumonia and the healthy on CXR images.

Material and Methods

Our study used anonymized data collected from public datasets. Therefore, institutional review board approval was waived according to regulations of our country.

Dataset

In the current study, two datasets were used: one dataset for CXR images of COVID-19 and the other for CXR images of the healthy and non-COVID-19 pneumonia. (I) The

COVID-19 image data collection repository on GitHub is a growing collection of CXR and CT images of COVID-19 pneumonia ¹⁶. In addition to COVID-19 pneumonia, this repository contains a small number of CXR and CT images of non-COVID-19 pneumonia.

(II) The RSNA Pneumonia Detection Challenge dataset available on Kaggle contains CXR images of non-COVID-19 pneumonia and the healthy ¹⁷. Figure 1 shows representative CXR images of COVID-19, non-COVID-19 pneumonia, and the healthy.

From the dataset (I), CXR images of lateral view and CT images were excluded, and CXR images of both posterior-anterior (PA) and anterior-posterior (AP) views were included. Based on these criteria, 215 and 33 CXR images were included from the dataset (I) for COVID-19 and non-COVID-19 pneumonia, respectively. In addition, 500 and 500 CXR images were randomly selected from the dataset (II) for the healthy and non-COVID-19 pneumonia, respectively. In order to avoid strong class imbalance, the 1000 CXR images were selected from the dataset (II). In total, 215, 533, and 500 CXR images of COVID-19 pneumonia, non-COVID-19 pneumonia, and the healthy were used for development and validation of the proposed method. From the two datasets, patient's age and sex were collected. Table 1 summarizes the patients' characteristics and CXR attributes. The 1248 CXR images were divided into 998, 125, and 125 images for training, validation, test sets, respectively. For image normalization, CXR images were divided by 255, and pixel

values of them ranged from 0 to 1.

Deep learning model and data augmentation

In the current study, VGG16¹⁸ was mainly used as deep learning model of the proposed method, and transfer learning was performed for the classification of CXR images of COVID-19, non-COVID-19 pneumonia, and the healthy. To search optimal hyperparameters of the VGG16-based model and combination of data augmentation methods, random search was performed in the current study¹⁹. Outline of deep learning model of the proposed method is shown in Figure 2.

Publicly available weights of VGG16 obtained by pretraining on ImageNet dataset were used for transfer learning. Transfer learning was performed by freezing the trainable parameters of 10 layers in VGG16. After the convolution layers of VGG16, global averaging pooling layer, fully-connected layer, and dropout layer, were added to VGG16. Final fully-connected layer with 3 unit was added after the dropout layer for the 3-category classification. Hyperparameters obtained by the random search of the VGG16-based model were as follows. Probability of the dropout layer was 0.1, and number of units in the first fully-connected layer was 416. We changed input image size of VGG16

to 220×220 pixels. The loss function was softmax loss. RMSprop with learning rate of 1.0×10^{-4} was used as the optimizer. The network was trained using a batch size of 8, and number of training epochs was set to 100. Early stopping was enabled using validation loss, and patience of early stopping was set to 7.

To prevent overfitting in the training of the model, optimal combination of the three types of data augmentation methods (conventional method, mixup, and RICAP) was also examined by the random search, and combination of conventional method and mixup were used in the proposed method of the VGG16-based model. The conventional data augmentation method included $\pm 15^\circ$ rotation, $\pm 15\%$ x-axis shift, $\pm 15\%$ y-axis shift, horizontal flipping, and 85%–115% scaling and shear transformation. The parameters of mixup was set to 0.1¹³.

The training of the model was performed on a PC with a discrete GPU (Nvidia RTX 2080 Ti, RAM 11 GB). Python (version 3.7, <http://www.python.org/>) was used as the programming language, and Keras (version 2.2.4, <http://keras.io/>) and TensorFlow (version 1.13.1, <http://tensorflow.org/>) were used as deep learning frameworks.

Comparison with other models and ablation study

To compare with the VGG16-based model, the following four pretrained models were

used for the transfer learning: Resnet-50 ²⁰, MobileNet ²¹, DenseNet-121 ²², and EfficientNet ²³. In the transfer learning using these four pretrained models, the trainable parameters of these pretrained models were not frozen; we found that the freezing of trainable parameters in these models degraded the model performance. For the four pretrained models, the random search was also performed to search optimal hyperparameters and combination of data augmentation methods. For EfficientNet, the best model was selected from B0–B7 by the random search.

To evaluate effectiveness of the data augmentation methods and the freezing of trainable parameters in the VGG16-based model, the following modified models were also evaluated for the VGG16-based model: (i) no data augmentation with the freezing, (ii) the conventional method only with the freezing, (iii) mixup only with the freezing, and (iv) the conventional method and mixup without the freezing.

Performance evaluation

For each model, performance evaluation was evaluated using the 3-category classification (ternary classification) accuracy of the test set with 125 images. To assure robustness of the models, the 3-category accuracy was calculated 5 times by changing random seed, training the models, and evaluating the test set. In addition, sensitivity of COVID-19

pneumonia was also calculated for the VGG16-based model.

Results

Table 2 shows the results of 3-category classification between COVID-19 pneumonia, non-COVID-19 pneumonia, and the healthy for the five pretrained models including the proposed method. The results were obtained by the random search to find the optimal hyperparameters and combination of data augmentation methods. According to Table 2, the mean accuracy of the VGG16-based model of proposed method was 83.7%. The mean accuracies of Resnet-50, MobileNet, DenseNet-121, and EfficientNet were worse than the VGG16-based model of propose method; the mean accuracies of these four models were less than 80%. The mean sensitivity of COVID-19 pneumonia was 90.9% for the VGG16-based model.

In Table 3, the effectiveness of the data augmentation methods and the freezing the trainable parameters was evaluated in the VGG16-based model. Table 3 shows that the layer freezing was effective. The combination of two types of data augmentation methods in the proposed method was more effective than single type or no data

augmentation methods. Although the combination of conventional method, mixup, and RICAP was also evaluated, the combination was not the best based on the results of random search. According to the results of random search, combination of conventional method and RICAP was slightly worse than the combination of conventional method and mixup. Therefore, the combination of conventional method and RICAP was not examined in the current study.

Discussion

Our results indicate that it was possible to construct the accurate CNN model by using both the transfer learning with VGG16 and the combination of data augmentation methods. Our results show that diagnostic accuracy of the 3-category classification between COVID-19 pneumonia, non-COVID-19 pneumonia, and the healthy was more than 80% in the proposed method. In addition, sensitivity of COVID-19 was more than 90%.

Table 3 shows that combination of two types of data augmentation methods was more effective than single type or no data augmentation methods. Our results were

compatible with the results of previous study for bone segmentation with CNN ¹⁵. Because the dataset of the current study was relatively small-sized (number of CXR images was 1248), it was necessary to improve the robustness of CNN models. For this purpose, the current study used the combination of data augmentation methods, and the combination of conventional method and mixup was most effective.

Among the several types of pretrained models, VGG16 was the most accurate for the 3-category classification. Although the classification accuracy of ImageNet dataset was higher in the other models than that in VGG16, our results were not compatible with the results of ImageNet dataset. Because the other models are more complicated (e.g., residual learning) and/or have a large number of trainable parameters, overfitting may occur in the current study with small-sized dataset. Effectiveness of the pretrained models in small-sized dataset should be further investigated.

The layer freezing for the trainable parameters was effective only in VGG16. Network architecture of VGG16 was simpler than that of the other models. For example, skip connection for residual learning in the other networks may hinder the layer freezing. This may affect the usefulness of layer freezing in CNN models.

As mentioned in the article of towardsdatascience.com ²⁴, several previous studies constructed datasets by adding pediatric CXR images of non-COVID-19

pneumonia to adult CXR images of COVID-19 pneumonia. However, when a CNN model is trained by these datasets, the model may try to distinguish between non-COVID-19 pneumonia and COVID-19 pneumonia by checking age differences between children and adults rather than disease differentiation. Therefore, in the current study, we included adult CXR images of the healthy and non-COVID-19 pneumonia from the RSNA dataset.

There are some limitations in our study. First, we developed and validated the proposed method using the public datasets. Overfitting may occur in external validation. Second, our CADx system was not used by clinicians. Clinical usefulness of our CADx system was not validated.

In conclusion, it was possible to build the accurate CADx system for the 3-category classification of COVID-19 pneumonia, non-COVID-19 pneumonia, and the healthy by the proposed method. The combination of two types of data augmentation methods was more useful than single type or no data augmentation methods.

Funding

The present study was supported by JSPS KAKENHI (grant number 19H03599 and JP19K17232).

Conflicts of Interest

The authors declare no conflict of interest. The funders had no role in the design of the study; in the collection, analyses, or interpretation of data; in the writing of the manuscript, or in the decision to publish the results.

References

1. WHO | Novel Coronavirus – China. *WHO*. 2020.
2. Stoecklin SB, Rolland P, Silue Y, et al. First cases of coronavirus disease 2019 (COVID-19) in France: Surveillance, investigations and control measures, January 2020. *Eurosurveillance*. 2020;25(6). doi:10.2807/1560-7917.ES.2020.25.6.2000094
3. COVID-19 situation reports. <https://www.who.int/emergencies/diseases/novel-coronavirus-2019/situation-reports>. Accessed May 27, 2020.
4. Fang Y, Zhang H, Xie J, et al. Sensitivity of Chest CT for COVID-19: Comparison to RT-PCR. *Radiology*. February 2020:200432. doi:10.1148/radiol.2020200432
5. Bai HX, Hsieh B, Xiong Z, et al. Performance of radiologists in differentiating COVID-19 from viral pneumonia on chest CT. *Radiology*. March 2020:200823. doi:10.1148/radiol.2020200823
6. Sodickson A, Baeyens PF, Andriole KP, et al. Recurrent CT, cumulative radiation exposure, and associated radiation-induced cancer risks from CT of adults. *Radiology*. 2009;251(1):175-184. doi:10.1148/radiol.2511081296

7. Wong HYF, Lam HYS, Fong AH-T, et al. Frequency and Distribution of Chest Radiographic Findings in COVID-19 Positive Patients. *Radiology*. March 2019:201160. doi:10.1148/radiol.2020201160
8. Yamashita R, Nishio M, Do RKG, Togashi K. Convolutional neural networks: an overview and application in radiology. *Insights Imaging*. 2018;9(4):611-629. doi:10.1007/s13244-018-0639-9
9. Nishio M, Sugiyama O, Yakami M, et al. Computer-aided diagnosis of lung nodule classification between benign nodule, primary lung cancer, and metastatic lung cancer at different image size using deep convolutional neural network with transfer learning. *PLoS One*. 2018;13(7):1-12. doi:10.1371/journal.pone.0200721
10. Chilamkurthy S, Ghosh R, Tanamala S, et al. Deep learning algorithms for detection of critical findings in head CT scans: a retrospective study. *Lancet*. 2018;392(10162):2388-2396. doi:10.1016/S0140-6736(18)31645-3
11. Rajpurkar P, Irvin J, Zhu K, et al. CheXNet: Radiologist-Level Pneumonia Detection on Chest X-Rays with Deep Learning. November 2017. <http://arxiv.org/abs/1711.05225>. Accessed January 8, 2020.
12. Tan C, Sun F, Kong T, Zhang W, Yang C, Liu C. A survey on deep transfer learning. In: *Lecture Notes in Computer Science (Including Subseries Lecture*

- Notes in Artificial Intelligence and Lecture Notes in Bioinformatics*). Vol 11141 LNCS. Springer Verlag; 2018:270-279. doi:10.1007/978-3-030-01424-7_27
13. Zhang H, Cisse M, Dauphin YN, Lopez-Paz D. mixup: Beyond Empirical Risk Minimization. *Polit Africaine*. October 2017:1-13.
<http://arxiv.org/abs/1710.09412>. Accessed May 27, 2020.
 14. Takahashi R, Matsubara T, Uehara K. Data Augmentation using Random Image Cropping and Patching for Deep CNNs. *IEEE Trans Circuits Syst Video Technol*. August 2019:1-1. doi:10.1109/tcsvt.2019.2935128
 15. Noguchi S, Nishio M, Yakami M, Nakagomi K, Togashi K. Bone segmentation on whole-body CT using convolutional neural network with novel data augmentation techniques. *Comput Biol Med*. 2020;121.
doi:10.1016/j.combiomed.2020.103767
 16. Cohen JP, Morrison P, Dao L. COVID-19 Image Data Collection. March 2020.
<http://arxiv.org/abs/2003.11597>. Accessed May 27, 2020.
 17. RSNA Pneumonia Detection Challenge | Kaggle.
<https://www.kaggle.com/c/rsna-pneumonia-detection-challenge>. Accessed May 27, 2020.
 18. Simonyan K, Zisserman A. Very deep convolutional networks for large-scale

- image recognition. In: *3rd International Conference on Learning Representations, ICLR 2015 - Conference Track Proceedings*. International Conference on Learning Representations, ICLR; 2015.
19. Bergstra J, Ca JB, Ca YB. *Random Search for Hyper-Parameter Optimization* Yoshua Bengio. Vol 13.; 2012. <http://scikit-learn.sourceforge.net>. Accessed May 27, 2020.
 20. He K, Zhang X, Ren S, Sun J. Deep residual learning for image recognition. In: *Proceedings of the IEEE Computer Society Conference on Computer Vision and Pattern Recognition*. Vol 2016-December. IEEE Computer Society; 2016:770-778. doi:10.1109/CVPR.2016.90
 21. Howard AG, Zhu M, Chen B, et al. MobileNets: Efficient Convolutional Neural Networks for Mobile Vision Applications. April 2017. <http://arxiv.org/abs/1704.04861>. Accessed May 27, 2020.
 22. Huang G, Liu Z, Van Der Maaten L, Weinberger KQ. Densely connected convolutional networks. In: *Proceedings - 30th IEEE Conference on Computer Vision and Pattern Recognition, CVPR 2017*. Vol 2017-January. Institute of Electrical and Electronics Engineers Inc.; 2017:2261-2269. doi:10.1109/CVPR.2017.243

23. Tan M, Le Q V. EfficientNet: Rethinking Model Scaling for Convolutional Neural Networks. *36th Int Conf Mach Learn ICML 2019*. 2019;2019-June:10691-10700. <http://arxiv.org/abs/1905.11946>. Accessed May 27, 2020.
24. Explainable AI and COVID-19 Chest X-rays | Towards Data Science. <https://towardsdatascience.com/investigation-of-explainable-predictions-of-covid-19-infection-from-chest-x-rays-with-machine-cb370f46af1d>. Accessed May 28, 2020.

Figures

Figure 1

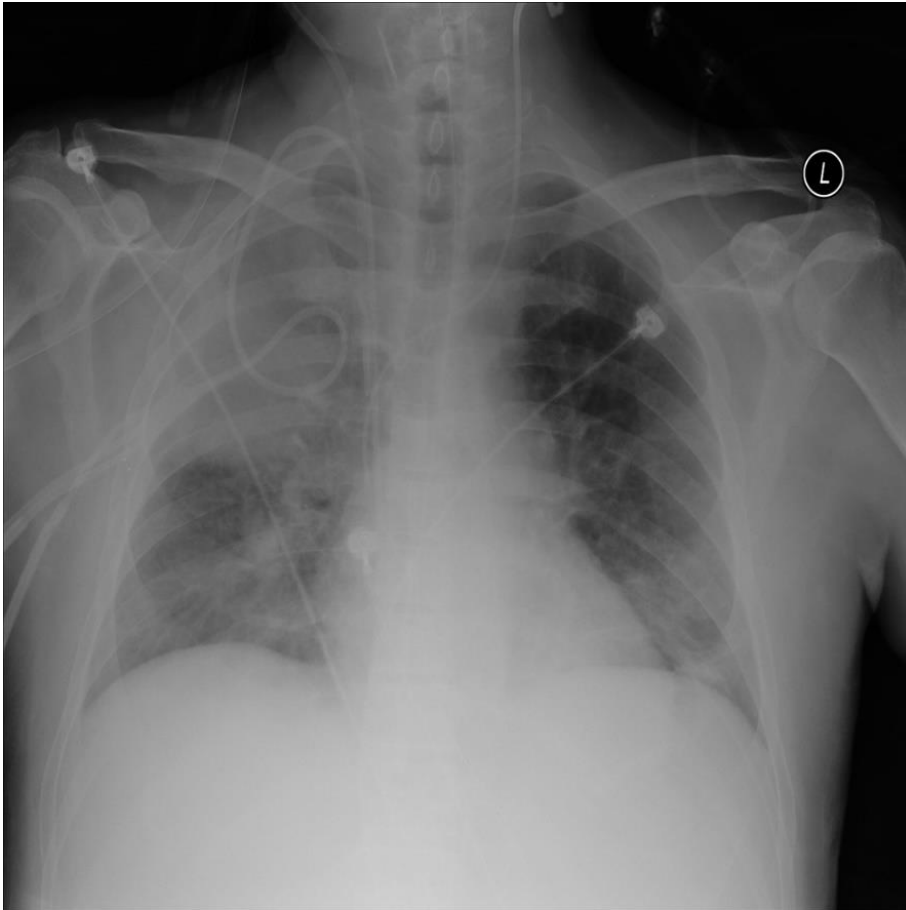
Representative CXR images of COVID-19 pneumonia, non-COVID-19 pneumonia, and the healthy

Abbreviations: chest X-Ray imaging (CXR), novel coronavirus disease (COVID-19)

(A) COVID-19 pneumonia of 30-year-old male



(B) non-COVID-19 pneumonia of 56-year-old male



(C) no pneumonia of 60-year-old female

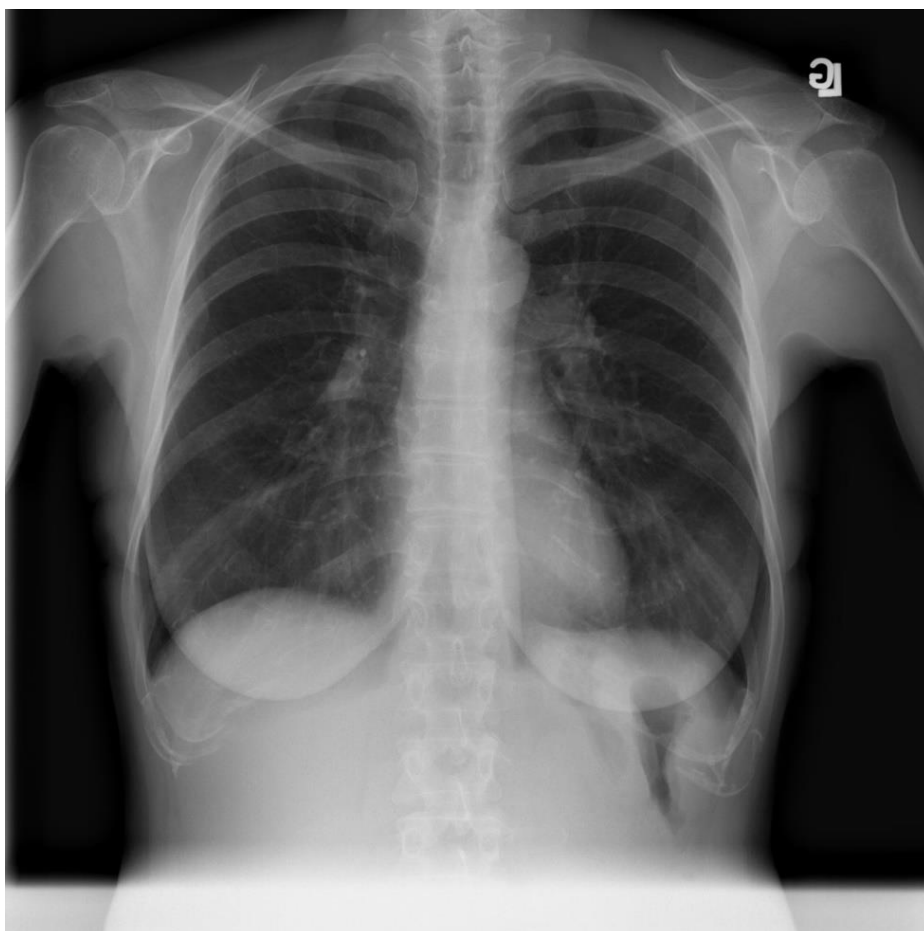
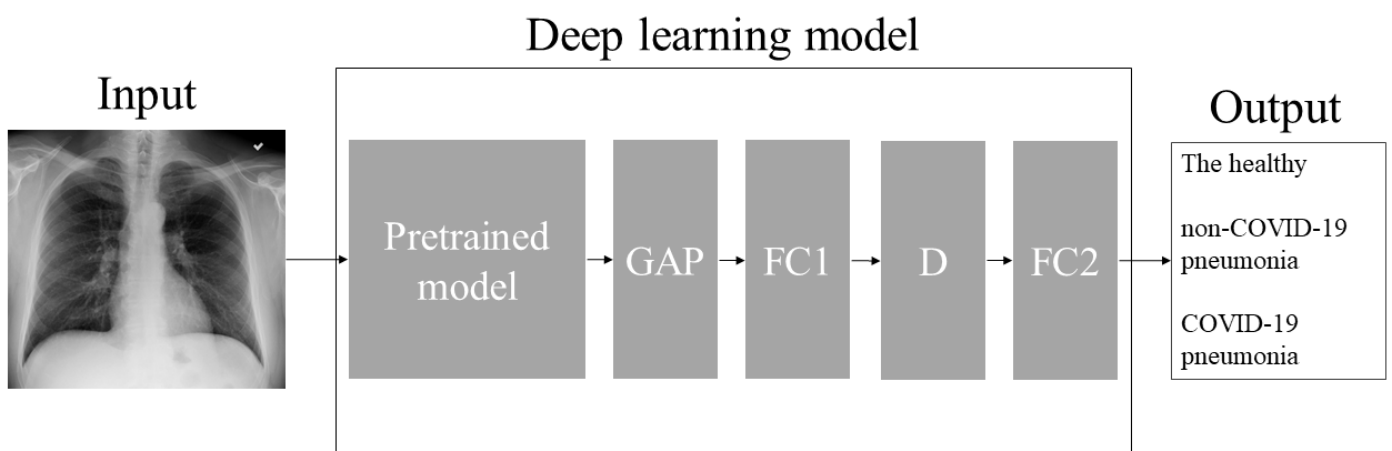


Figure 2

Outline of deep learning model of the proposed method

Note: For pretrained models, VGG16, Restnet-50, MobileNet, DenseNet-121, and EfficientNet were used in the current study.

Abbreviations: global averaging pooling layer (GAP), fully-connected layer (FC), dropout layer (D)



Tables

Table 1

Patients' characteristics and CXR attributes.

Category	Value
Number of images	1248
Sex	
Male	512
Female	702
Not available	34
Age	
Available	1205
Not available	43
Mean \pm SD of age (years)	48.1 \pm 17.5
Diagnosis	
COVID-19	215
non-COVID-19 pneumonia	533
the healthy	500
CXR view	
PA	666
AP	582

Abbreviations: chest X-Ray imaging (CXR), novel coronavirus disease (COVID-19), standard deviation (SD), posterior-anterior view (PA), anterior-posterior view (AP).

Table 2

Results of five deep learning models

Models	Loss of test set	3-category accuracy of test set
VGG16 (proposed method)	0.4682 ± 0.0289	0.8368 ± 0.0200
Restnet-50	0.5237 ± 0.0161	0.7776 ± 0.0118
MobileNet	0.4919 ± 0.0300	0.7872 ± 0.0322
DenseNet-121	0.5276 ± 0.0082	0.7824 ± 0.0223
EfficientNet	0.5206 ± 0.0177	0.7840 ± 0.0182

Note: Value of each cell was mean \pm standard deviation of 5 trials.

Table 3

Results of ablation study of the proposed method for data augmentation methods and layer freezing

Models	Loss of test set	3-category accuracy of test set
Proposed method	0.4682 ± 0.0289	0.8368 ± 0.0200
no data augmentation with layer freezing	0.9009 ± 0.1967	0.7872 ± 0.0165
conventional data augmentation method only with layer freezing,	0.4863 ± 0.0274	0.8256 ± 0.0245
mixup only with layer freezing	0.6407 ± 0.0674	0.7920 ± 0.0175
conventional data augmentation method and mixup without layer freezing	0.5143 ± 0.0179	0.7904 ± 0.0260

Note: Value of each cell was mean \pm standard deviation of 5 trials.

Table 4

Representative confusion matrix of 3-category classification in test set

		Prediction by the proposed model		
		the healthy	non-COVID-19 pneumonia	COVID-19 pneumonia
Ground truth	the healthy	43	7	0
	non-COVID-19 pneumonia	9	41	3
	COVID-19 pneumonia	2	0	20

Note: Accuracy was 83.2% (104/125).